Mitigating Power and Memory Constraints on a Venusian Seismometer

Yuan Tian[*1], Robert R. Herrick[1], Michael E. West[1], and Tibor Kremic[2]

Abstract

The nearest term pathway to the deployment of a seismometer on Venus is an instrument that can operate under ambient surface conditions on battery power. We conduct a series of studies on combined hardware and software approaches to maximize the quality of data returned under the likely restrictions of minimal on-board data storage and only being able to transmit in real time during a small fraction of a multimonth deployment. We assess likely Venus seismicity by examining different terrestrial analog settings; we find that likely Venus analog settings all fall within about an order of magnitude of mean Earth in terms of seismicity level. We use the seismic record from a station in central Alaska as a Venus surrogate for algorithm development. We tested various transmission triggers and developed a simple low-memory algorithm that mimics the common terrestrial long-term average/short-term average trigger. If the seismometer can operate in coordination with an orbiter that can remotely turn off data transmission, then the frequency content of a few seconds of data can be used to distinguish small, nearby earthquakes from large, distal ones, and total data transmission can be tuned to favor the latter. If an orbiter can also turn on transmission for other nearby seismometers, it would further enhance the ability to distinguish small- and large-magnitude earthquakes autonomously and increase the chances of capturing the initial onset of significant events.

Introduction

Seismology is the preeminent methodology for studying the structure and composition of a planet's interior (Lognonné and Johnson, 2007; Banerdt *et al.*, 2020; Lognonné *et al.*, 2020; Tian and Zheng, 2020). The behavior of seismic waves traveling through planetary bodies provides constraints on interior composition, compositional boundaries and transitions, and the state of the material (e.g., fluid versus solid, hot versus cold, and porosity). Thousands of seismometers have been deployed on Earth, a few were deployed on the moon by the Apollo missions (Nakamura *et al.*, 1982), and the InSight mission (Banerdt *et al.*, 2020) deployed a currently operating seismometer on Mars. Seismometers were also attached to Viking (Mars) and Venera (Venus) landers but recorded no data unambiguously attributable to earthquakes.

Using seismology to understand the interior of Venus is a high scientific priority. The similar size of Venus and Earth, and their similar overall surface ages (McKinnon *et al.*, 1997; Herrick and Rumpf, 2011), suggest that Venus should have a level of seismic activity comparable to Earth's and much higher than the moon or Mars. However, Venus has some fundamental differences from Earth. Foremost among these is the observation that while Venus exhibits abundant evidence of folding and faulting on the surface, the planet does not currently have Earth-like plate tectonics (Solomon *et al.*, 1992). There have been a variety of big-picture geodynamic models for Venus put forth to explain its different distribution and nature of volcanism and tectonic deformation (e.g., Turcotte, 1993; Basilevsky and Head, 1995; Solomatov and Moresi, 1996; Guest and Stofan, 1999; Herrick, 1999; Johnson and Richards, 2003; Byrne *et al.*, 2021). Some scenarios predict a varying level of surface geologic activity with time and would have Venus's current tectonic activity low and akin to Earth's cratonic regions (e.g., Turcotte, 1993; Basilevsky and Head, 1995), whereas other scenarios suggest that current tectonic activity is different in style but similar (or even greater) in level to Earth (e.g., Guest and Stofan, 1999; Byrne *et al.*, 2021).

A workshop in 2014 (Stevenson *et al.*, 2015) brought together several seismologists to discuss the Venus seismicity. Some participants felt that the overall higher temperatures of the uppermost crust on Venus (surface temperature ~450°C) might make most fault movement aseismic, although the

1. Geophysical Institute, University of Alaska Fairbanks, Fairbanks, Alaska, U.S.A., https://orcid.org/0000-0002-8621-088X (YT); https://orcid.org/0000-0002-0974-6293 (RRH); 2. National Aeronautics and Space Administration, Glenn Research Center, Cleveland, Ohio, U.S.A.

*Corresponding author: ytian4@alaska.edu

consensus at the workshop was that the elevated surface temperature probably plays a minimal role in affecting overall seismicity. The absence of water in the near surface of Venus could also potentially affect the nature of seismicity, as could the higher surface air pressure. To our knowledge there is no straightforward way to treat the effects of differing near-surface water content, temperature, and pressure conditions on the nature and level of seismicity, and we see no clear reason why Earth–Venus differences in these parameters would be important, so we do not treat them in this work.

Because of the high surface temperature on Venus and the limited solar energy reaching the surface relative to the power needed to transmit data, the option of placing solar-powered seismometers on the surface for an indefinite period, as has been done on Mars and the Moon, is not currently a viable option (Venus Exploration Analysis Group [VEXAG], 2019). The longest that a surface lander with conventional electronics has lasted on the Venusian surface is about two hours. Yet to accomplish even the most basic goal of determining seismicity levels requires the ability to operate over a period of at least days. Although nuclear power might be viable for either active cooling or simply as a long-lived power source, regulatory and cost considerations are such that here we do not consider its use for seismology on the Venus surface (VEXAG, 2019).

Over the past several years research and development of high-temperature electronics has advanced to the point in which a seismometer that can operate under Venus ambient conditions using battery power has become technically feasible (Kremic et al., 2020). There is not currently a functioning prototype for a Venus seismometer, although one is currently under development as part of the National Aeronautics and Space Administration High Operating Temperature Technology program. What exists are high-temperature-compatible alternatives to many of the electronic and mechanical parts that would go into a seismometer, and an understanding of the state of the field of high-temperature electronics sufficient to reasonably predict the capabilities of what could be brought to fruition in the next few years. A major part of the rationale for the work presented here is a desire to anticipate how the instrument will operate on Venus to help guide and prioritize future development, such as the ongoing High Operating Temperature Technology program. This will be an iterative process moving forward.

The constraints on operation of a first-generation seismometer on Venus will be severe. The battery will likely be capable of enabling the seismometer to operate for a period of a handful of months (Glass et al., 2020; Kremic et al., 2020). However, transmission of data from the surface to a relay orbiting spacecraft will be power intensive, such that less than ten hours of data will likely be able to be transmitted from the surface. Because data transmission rate depends in part on transmitter power, it may be the case that frequency and dynamic range of the instrument will be limited to less than instrument capability. Furthermore, although limited computer memory is being developed for high-temperature devices, power consumption will be high, such that storing even small amounts of data for later transmission may not be possible in the near term.

There are alternatives to a surface seismometer that are being explored by others that may be able to evaluate current aspects of Venus seismicity. The high density ($\sim$65 kg/m^3) and pressure (90 bars) of the atmosphere at the surface–atmosphere boundary means that good coupling should occur, so observing earthquakes using infrasound from a balloon platform in the atmosphere should be possible (Krishnamoorthy et al., 2020). Modeling also suggests the possibility of observing from orbit wave propagation from large earthquakes in the upper levels of the atmosphere (Didion et al., 2018). Although both the ideas hold promise for long-term continuous monitoring, interpreting the data from such instruments relies on an understanding of Venus seismicity that we do not currently possess. Interpreting data from aerial or spaceborne observations requires removing distortions and noise produced in the atmosphere, a daunting challenge without having existing knowledge of the seismicity as observed at the surface. Ideally, both the methods would be calibrated by collecting data during simultaneous observation with a surface seismometer.

In the work here we present a series of initial case studies designed to develop and assess methods for dealing with some of the limiting constraints on a Venus surface seismometer. We will operate under the assumption that a battery could power a seismometer operating on the Venusian surface for a period of a few months, but during that time it will only be able to transmit a few hours of data back to an orbiting spacecraft (and then back to Earth). In general terms, if we consider a "typical" large-scale seismic event as requiring ten minutes of data transmission, then we can think of the seismometer as being capable of transmitting 50 events before the battery is drained, which is in family with the number of events expected over a Venus solar day (Lorenz, 2012). The overall goal, then, is to develop feasible hardware and software solutions that will enable the seismometer to autonomously select the "best" few hours of data to transmit during its multiple months of operation. Our desires then can be described as follows:

- Transmit data only from clear earthquakes and do not transmit wind noise.
- Tune sensitivity of any transmission trigger so that only relatively strong events are transmitted, such that a mean of approximately one event every other day gets transmitted.
- Skew the seismometer to preferentially favor transmitting large, farther away earthquakes over nearby small earthquakes that produce similar amplitude signals. The more distal earthquakes provide more information about regional- and global-scale seismicity and can be used to infer planetary interior structure.

The studies that we performed are as follows. First, we estimated an overall seismicity level for Venus and identified

TABLE 1
Number of Earthquakes Over M_w 5 per Area per Year

Region	Earth Average	East Africa Rift Zone	Caribbean Plate	Alaska Interior	Earth Average, Excluding Plate Boundaries
Seismicity density (10^{-7} km^{-2} yr^{-1})	36.0	16.62	39.79	2.7	2.7

The fact that the quieter parts of Earth are still within an order of magnitude of the Earth average provides some confidence that designing a seismometer to our best guess of Venusian analog conditions will yield acceptable results in practice.

reasonable Earth analog sites that can be used as test areas for potential seismometer designs. After settling upon a suitable analog setting, we thoroughly characterized a multiday seismic record from an analog site, noting the time, location, and magnitude of every seismic event recorded at our test site. Using the resulting cataloged record, we then evaluated the performance of the seismometer operating under the likely constraints imposed by Venus's surface conditions. We examined the effects of different band-pass filters on our ability to detect earthquakes and separate them from noise.

To optimize data return, we designed and assessed the performance of a couple of data transmission triggers. A simple threshold trigger for data transmission was analyzed by studying the effects of its tunable parameters. A threshold trigger is easy to implement and requires no data storage on the seismometer. We also developed a trigger that is feasible with expected lander constraints that we call the "segmented window" trigger. This trigger approximates a commonly used terrestrial trigger—the short-term average/long-term average trigger (ratio of STA/LTA; Trnkoczy, 2009).

Because these triggers need to detect the first moments of a seismic event, they have minimal ability to distinguish between small nearby events and the more interesting larger but farther away earthquakes. However, in a scheme in which the computer on an orbiting satellite could autonomously analyze data from a seismometer, or even a network of seismometers, it may be possible that after a short period of time to distinguish between small- and large-magnitude events and then cease transmission from smaller events, thereby enabling more large events to be transmitted with limited battery power. Thus, we include some initial thoughts on rapid autonomous analysis approaches that might be used in this capacity.
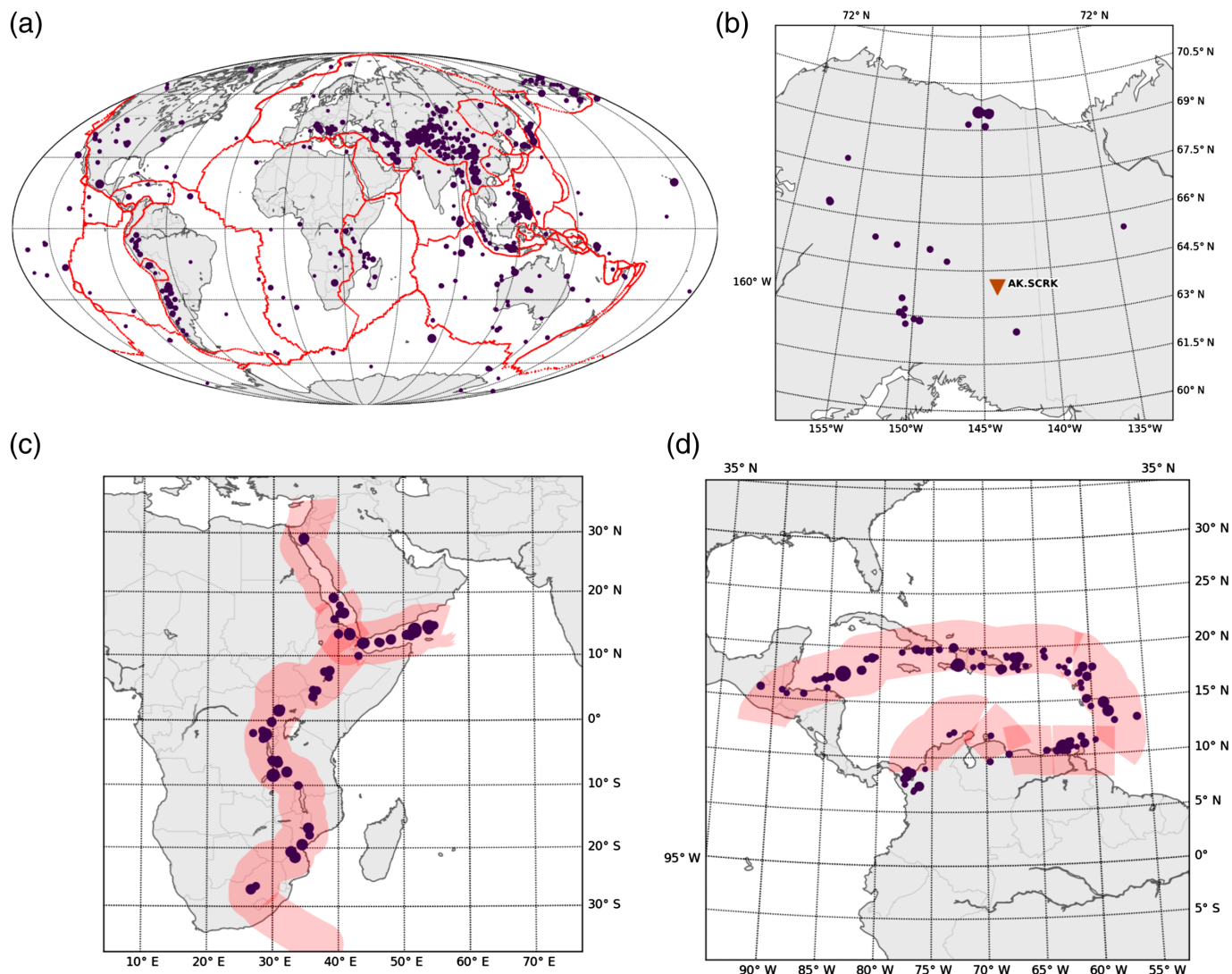
Venus Seismicity Estimation

Our desire is to test seismometer design, including triggering mechanisms, against our best estimate of likely Venus conditions. We begin by estimating the nature and level of seismicity on Venus. Although there are differences between Venus and Earth's lithospheric structure and tectonic styles, there are some areas on Earth that have been suggested as Venus analogs. The African plate has no subduction zone boundaries, minimal movement relative to the hotspot reference frame, and some limited extension along the East Africa rift; its hotspot-dominated tectonics and volcanism has been suggested as the overall setting

on Earth's most analogous to Venus (Burke, 1996; Herrick, 1999). Some large coronae on Venus may have retrograde subduction (Sandwell and Schubert, 1992), and the Caribbean plate region has been suggested as an analog (Davaille et al., 2017). Because some proposed geologic histories for Venus have been proposed that make present-day Venus relatively quiescent (Basilevsky and Head, 2002), some of Earth's intraplate areas may also be reasonably analogous settings.

Besides the spatial distribution of the earthquakes on Venus, the magnitudes of a typical sampling of earthquakes might also be different than for Earth. For example, if Venus is truly a one-plate planet, and earthquakes are only caused by thermoelastic stresses, then by analogy with Earth the maximum moment magnitude would be ∼6.5 (Lognonné and Johnson, 2007). We note that in our test data discussed in the Analog seismicity catalog section that the time period selected had no earthquakes above moment magnitude 7.0 and only a few above moment magnitude 6.5. Thus, even if the hypothesis is correct that no earthquakes above moment magnitude 6.5 are possible, it does not significantly alter the conclusions from the tests that we are performing.

In Table 1 and Figure 1, we compare the mean seismicity of Earth to some of the Venus analog settings, and we show the mean Earth excluding earthquakes within two degrees (222 km) of a designated plate boundary. Overall, quiet places on Earth are within an order of magnitude or so in terms of seismicity compared to regions near plate boundaries. This provides some confidence that designing to a level of seismicity found in these quiet places will not be drastically different from Venus. The Caribbean plate is a well-monitored and well-understood example of rollback subduction; the overall seismicity level likely includes some contributions on the eastern end from Pacific plate subduction and, thus, is likely a modest overestimate. The portions of the East Africa rift system that were chosen have been previously noted for their resemblance to rifting in Beta Regio—part of the globe-encircling Venusian rift systems (McGill et al., 1981; Foster and Nimmo, 1996).

The initial InSight results for Mars (Banerdt et al., 2020) were interpreted to indicate a seismicity level a few hundred times lower than global Earth (this involved extrapolating observations from the InSight location to a global estimate). Given the considerably more faulted and fractured surface of Venus compared to Mars, it seems reasonable to expect Venus to be at least an order of magnitude more active than Mars. The (Banerdt et al., 2020) article also includes an interpretation of

Figure 1. Intraplate events greater than M_w 5 in 2010–2020. The dots represent seismic events; dot size shows magnitude of events ranging from M_w 5 to 9. (a) Red lines show major plate boundaries, and all events shown are more than 2 degrees from a plate boundary. The seismicity density of events greater than M_w 5 is about 2.7 per million square kilometer per 10 yr. (b) All large events in the Alaska interior (a circle centered at 67° N, 145° W, and radius 5°). The seismicity density of events greater than M_w 5 in the region is also about 2.7 per million square kilometer per 10 yr. The red triangle is the station we have chosen for a Venus analog for the testing in the subsequent sections. (c) The seismicity in the east Africa rift zone; the pink shading shows the area used for the spatial density calculation. (d) The seismicity near the Caribbean plate boundary. The pink shading indicates the area near the plate boundary used in the spatial density calculation of Table 1. The color version of this figure is available only in the electronic edition.

(Okal *et al.*, 2007) to arrive at estimates of intraplate seismicity for "tectonically deformed regions away from plate boundaries" and "stable continental interiors," with the former around 35 times lower than global Earth and the latter about 200 times lower. The (Okal *et al.*, 2007) was focused on evaluating whether the magnitude distributions between intra- and interplate earthquakes are similar (their conclusion was that they are), and the values shown in (Banerdt *et al.*, 2020) are a repackaging of their results. The larger global to intraplate ratio on Earth than we found is primarily from Okal *et al.* (2007) using different starting catalogs than we did, excluding earthquakes to a farther distance from plate boundaries and subtracting hotspot-related seismicity. In short, we think this previous work is also supportive of the best guess of a Venus seismicity level ten to twenty times lower than Earth and of using a seismometer in an intraplate setting as a Venus analog.
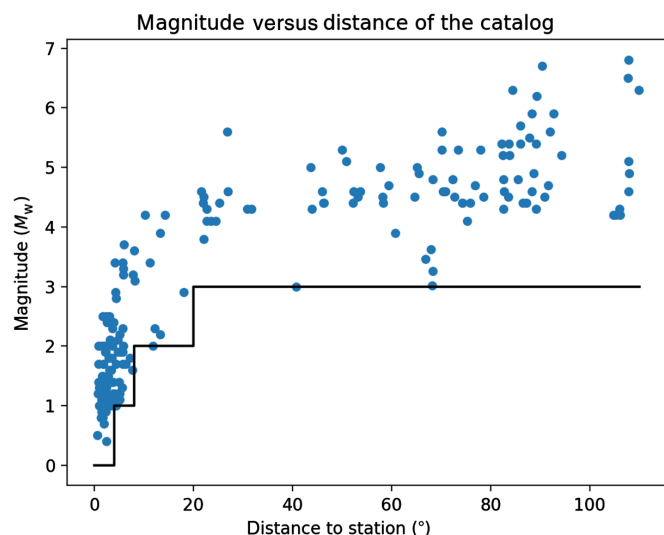
Analog Seismicity Catalog

We took a multiday seismic record located in a Venus analog setting, and comprehensively documented and characterized the different types of seismic signals in the record beyond just cataloged events. We used this catalog to evaluate the efficacy of filtering and triggering mechanisms. We chose a 9-day record

Figure 2. Event magnitude versus epicenter distance for the benchmark catalog. The blue dots are representing events in the catalog. The black line is a manually selected line for the minimum magnitude searched in each distance. The color version of this figure is available only in the electronic edition.

from a station located in central Alaska from a period with no global major (M_w 7+) earthquakes and associated aftershocks (labeled in Fig. 1 as AK-SCRK, "AK" for the network and "SCRK" for the station code). Based on the Venus seismicity estimation section, central Alaska is an intraplate region that we interpret to be an acceptable Venus analog setting. We chose this station in part, because the authors have a good understanding of the setting; and, thus, we can identify and characterize the various nonearthquake environmental signals.

The catalog is constructed in several steps, combining a recursive STA/LTA method, manual picking, and machine learning (Fig. 2):

1. We applied some initial constraints based on distance and events magnitudes to the global seismic events catalog (the black line in Fig. 2).
2. We used a recursive STA/LTA method to generate detections on nine days of continuous data.
3. We used the machine learning-based detection package EQTransformer (Mousavi et al., 2020) to detect nearby events and combine them with the events detected by the recursive STA/LTA method implemented via ObsPy (Megies et al., 2011; Wassermann et al., 2013).
4. We calculated the theoretical arrival time of all events in the catalog using a TauP algorithm (Crotwell et al., 1999).
5. We next associated the detections with catalog events based on their arrival time.
6. Finally, we manually checked each associated event as a quality control. These associated events compose our catalog. For each event in the catalog, we have entries for

location of the event, magnitude, distance to the single station, event type, and the origin time.

The relationship between magnitude and distance of all the events in the catalog is plotted in Figure 2. As would be expected, the catalog contains many small events that occurred near the station, and only large events from farther away are detectable above the station noise.
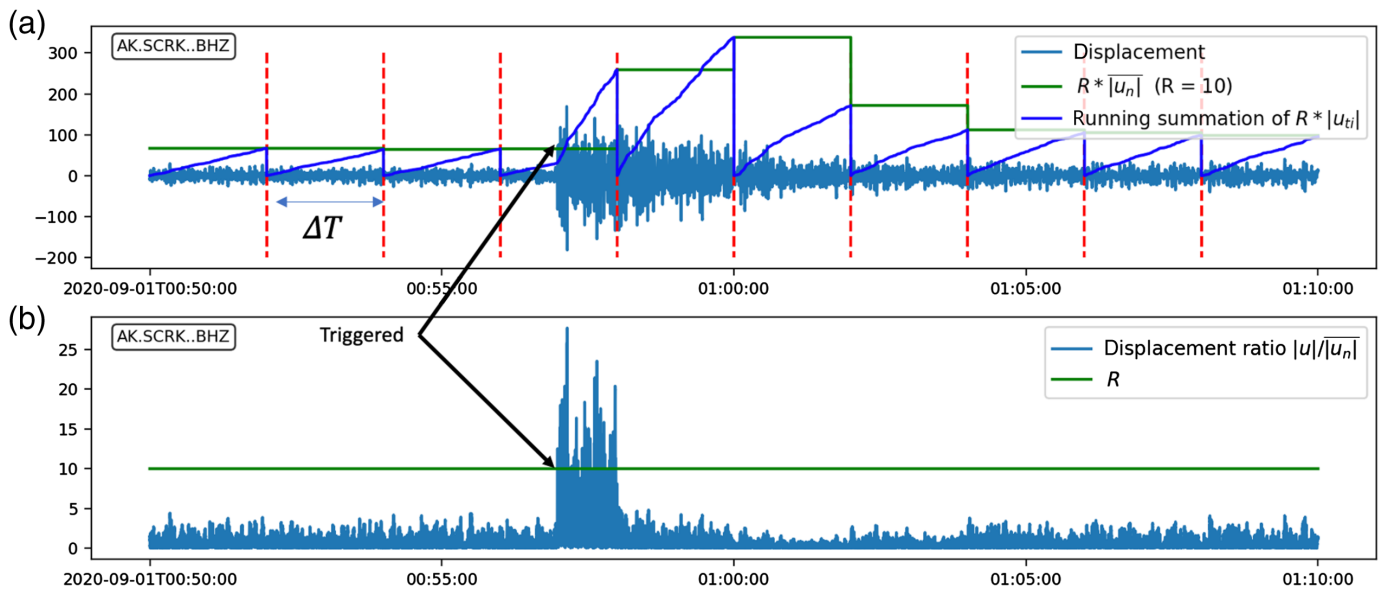
Seismicity Detection Method

Because both data storage and data transmission are power intensive, we desire a data transmission trigger that is accurate (triggers on real events and does not trigger on noise) and requires no more than a few bytes of storage. This requirement rules out the common STA/LTA trigger, which requires storing a rolling time window of data. Here we test two transmission triggers—an amplitude threshold and a low-memory method designed to mimic the STA/LTA trigger that we call the "segmented window" method. In the testing that we present in this section, we assume that after triggering the seismometer transmits data for a fixed period of time. In the preliminary seismometer design presented in Kremic et al. (2020), a transmission interval of 10 min was suggested. In the Discussion section, we consider the possibility of being able to send a "stop-transmission" signal to the seismometer.

The amplitude threshold method we use has two parameters: the "threshold", the amplitude value that triggers seismometer transmission; and the "minimum trigger interval", which is the minimum time between two triggers and can obviously be no smaller than any specified post-triggering transmission period. Setting the minimum trigger interval parameter at several times the transmission period helps reduce the amount of bad data transmitted during a high-noise period at the seismometer. For example, if the transmission period is 10 min and the minimum trigger interval is 30 min, then during a one-hour period of high-amplitude wind noise that would continuously trigger transmission we would only transmit a total of 20 min. Because the minimum trigger interval increases, however, the ability to detect earthquakes close in time is necessarily diminished.

The primary advantage in functionality that the STA/LTA method has over a simple amplitude threshold method is that it adjusts the sensitivity to account for changes in ambient noise. If noise levels become high, then only the larger earthquakes would produce an adequate signal-to-noise ratio to trigger transmission. An example of a situation that the STA/LTA method would handle effectively is the diurnal variation in wind noise levels observed on Mars at the InSight seismometer (Giardini et al., 2020).

To better mimic STA/LTA performance, we designed an approach that does not require storage of a rolling time period of data. We call this the "segmented window" method. Compared to the amplitude threshold, this method has only

Figure 3. Illustration of the "segmented window" method. (a) The displacement seismogram $u(t)$ is from the Z component of broadband seismometer SCRK. The seismogram is divided into windows of length $\Delta T = 120$ s (red dashed lines). The green line is mean window noise, $|\overline{u_n}|$, multiplied by the threshold value (multiplying by the threshold R makes it possible to observe directly when the displacement $|u_{t_i}|$ triggers). The running summation of $R \times |u_{t_i}|$ is plotted as blue solid line. This summation can be performed continuously to compute the mean absolute displacement for use during the next time window. (b) The displacement ratio $\overline{|u_{t_i}|/|\overline{u_n}|}$. The adjustable threshold R is plotted in solid green line. The color version of this figure is available only in the electronic edition.

three more parameters, which means it requires very little extra memory on a seismometer. This approach first divides the seismic record into equal length time windows (ΔT) (Fig. 3). The seismometer only stores the cumulative summation of the most recent full window. We can then get the mean absolute value of the data $|\overline{u_n}|$ in that window by dividing by the number of samples, where $|\overline{u_n}| = \frac{\sum_{t_n-\Delta T}^{t_n}|u_{t_i}|}{N_{\Delta T}}$, ΔT is the window length, $t_n - \Delta T$ is the starting time of the window, $|u_{t_i}|$ is the absolute value of the seismic record for sample t_i, and $N_{\Delta T}$ is the number of samples in the window. This mean describes the noise level of this period of time. The ratio $\overline{|u_{t_i}|/|\overline{u_n}|}$ is then a running measure of the signal amplitude relative to the most recent segmented window. This ratio functions as a type of signal-to-noise measure. Therefore, we can set a ratio-based threshold, R, instead of setting a constant threshold throughout the recording. Once the displacement reaches this ratio-based threshold, the seismometer will be triggered for a certain amount of time (30 min in this example). This method can help prevent the seismometer from falsely triggering when the data is noisy. One way to implement the segmented window is to store only $|\overline{u_n}|$ from the previous time window, the running summation of $|u_{t_i}|$ in the current time window, and a time marker of when the current window ends. With this minimal addition of required memory, the segmented window method has a superior performance when there is high frequency noise (Fig. 4).
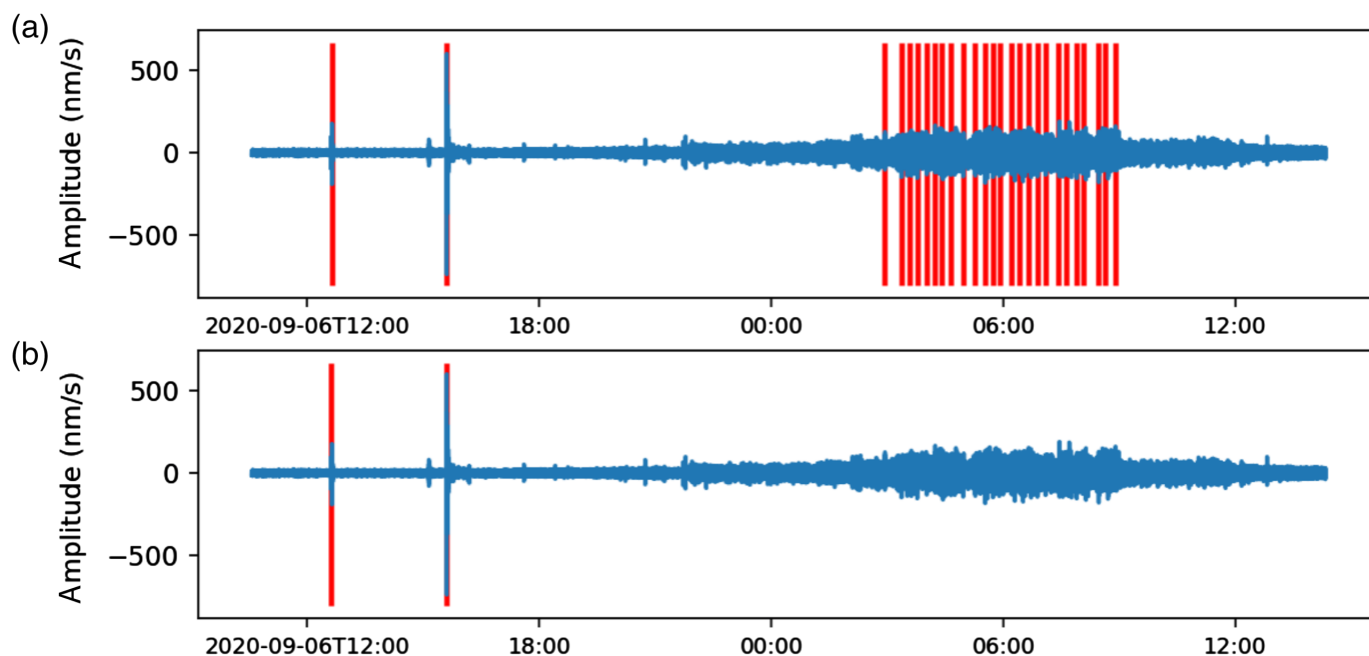
Algorithm Performance

We define success as triggering on as many real events in the catalog as possible without triggering on noise. We evaluate our two low-memory approaches and benchmark them against a traditional STA/LTA approach. We adjusted the sensitivity to increase or decrease the number of triggered events when used with our seismicity catalog. To fairly compare the performance

of different method, we set the minimum trigger interval of both the approaches at 30 min and test against the same nine-day record. We preprocess the waveforms with a 0.8 Hz high-pass filter to improve the ability to detect initial body waves. If a similar filter were to be used in the onboard trigger algorithm, it could be integrated into the electronics and would not need to consume digital resources. The event association is based on the triggered time and the first arrival time of cataloged events estimated using the TauP method (Crotwell *et al.*, 1999). If an event arrival time in the catalog is within the interval from 80 s before to 10 s after a triggered time, we consider an event in the catalog to have been correctly triggered. We then determined the fraction of the trigger events that were correct detections (Fig. 5a).

For all the three trigger mechanisms, the number of detections obviously increases as we lower the threshold (threshold detection method) or the ratio (STA/LTA and segmented window). The percentage of successful detections (true positive rate) of threshold detection method drops rapidly with decreasing threshold value but stays above 75% for a wide range of ratios with the other two triggering methods, eventually dropping as the ratio approaches 1. We also computed the "false positive

Figure 4. (a) Comparison of the amplitude threshold detection algorithm and (b) the segmented window detection algorithm. Vertical red lines show when the algorithm indicated detection of an earthquake. The latter half of this record includes considerably high frequency noise. The color version of this figure is available only in the electronic edition.

rate" and the "true negative rate" for comparing the performance of these three methods (Fig. 5b,c).

Other parameters also impact the overall performance. The minimum rest interval between detections affects the number of detections, with longer rest intervals decreasing the number of detections. As we discuss subsequently, noise and earthquakes have a range of frequency characteristics, so our choice of frequency filter before implementing a trigger significantly affects performance. From our observation, small events can often hide beneath the low-frequency surface waves of large earthquakes. The frequency spectrum of noise sources like wind tend to skew toward high frequencies, ∼8–25 Hz. But these effects could be mitigated with a band-pass filter.

We conducted a parameter space exploration to determine the influence of the minimum trigger interval and various band-pass filters. With the threshold method, the ratio of correctly detected events is typically very low if the threshold is low. However, by increasing the minimum trigger interval, we can minimize false triggers (Fig. 6).
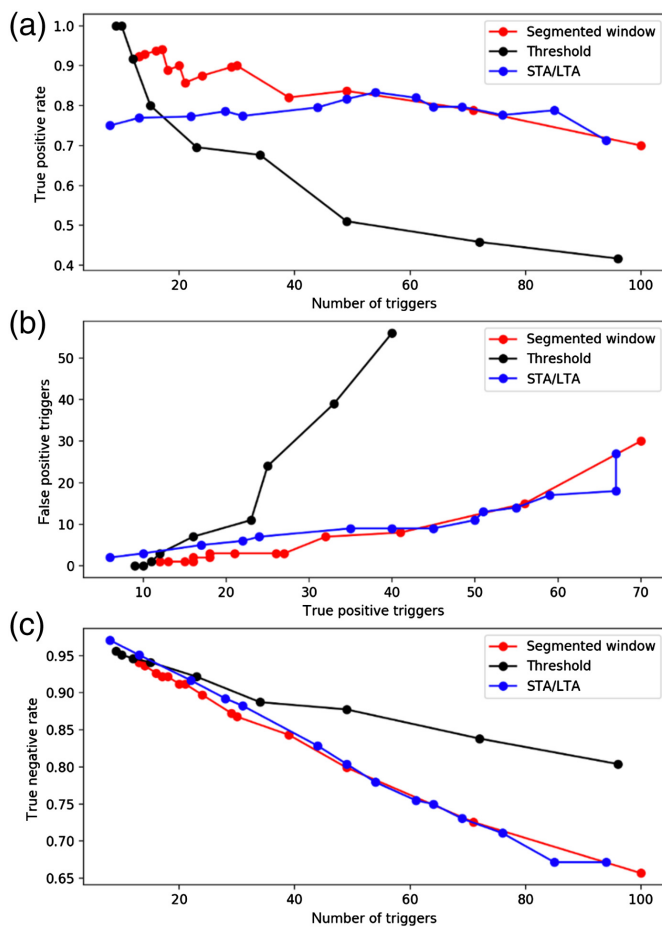
As discussed earlier, it is important to examine the effect of a band-pass filter on our seismic events detection. The lower frequencies provide the most information on deep structure and are important for separating large, distal earthquakes from nearby small ones. The higher frequency limit can help us know what sampling rate is optimal for the Venus seismometer. The higher the sampling rate of the seismometer, the more power is required to transmit data to an orbiter. The required sampling rate is determined by the highest frequency being recorded, so we are strongly motivated to set the high-end of a band-pass filter to the lowest value that does not significantly alter the interpretability of the data. Figure 7 explores band-pass filtering effects for the direct threshold and segmented window methods. For the threshold method there is

no choice of filters that does a particularly good job of triggering on large numbers of earthquakes with a high percentage of detections. However, using the segmented window with a band-pass of around 2–8 Hz (black star) maximizes both the number of detections and the percentage that are accurate.

Separating Large, Farther Away Events from Small Nearby Ones

If a seismometer on Venus is fortunate enough to detect more earthquakes than can be transmitted, then our preference would be to prioritize larger earthquakes that are coming from farther away from the lander; they provide more information about the deep interior and global tectonics. The triggering methods cannot evaluate whether a first break is from a small, nearby event or a large, farther away event. However, this may be possible using a short time series of data (perhaps just a few seconds). Thus, if orbiter–lander communications provide the ability to tell a seismometer to stop transmitting, autonomous processing on the orbiter might be able tell the seismometer to transmit a long time for distal earthquakes but only transmit a short time for nearby earthquakes. We have explored three methods that may be able to distinguish between distal and nearby events rapidly and autonomously. The methods rely on the general observation that the larger, more distal earthquakes should have relatively more low-frequency signal content than small nearby events. Each method processes an initial portion of the seismic

Figure 6. Exploration of parameter space of threshold detection method. The horizontal axis is the minimum trigger interval, which is the minimum time allowed between two triggers. The vertical axis is the value of threshold. The color version of this figure is available only in the electronic edition.
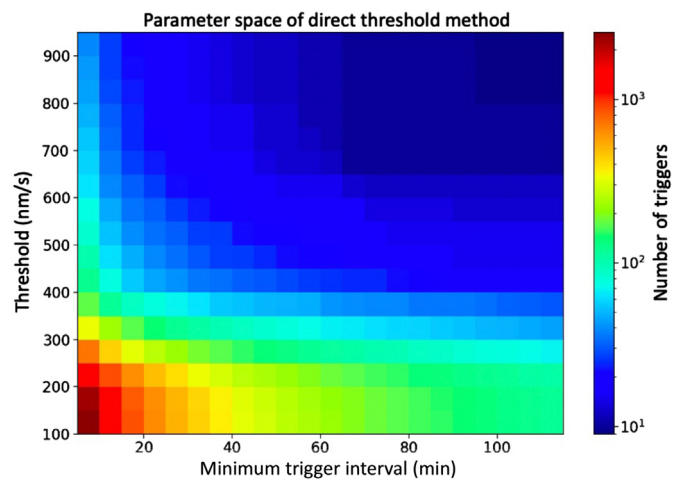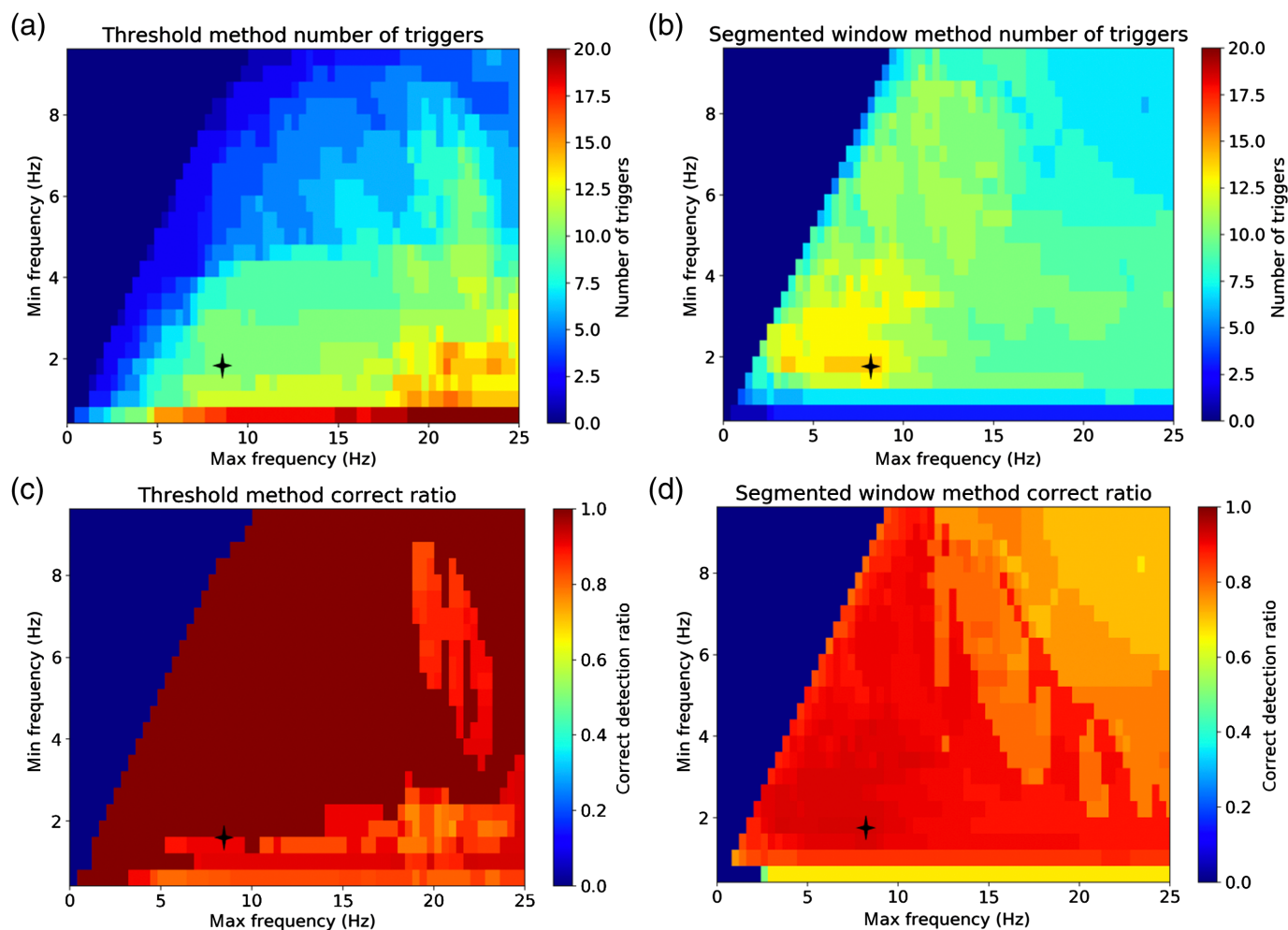
Figure 5. Comparison of three detection algorithms in terms of successful detections and false positives as the sensitivity of the algorithms are adjusted to increase the number of triggers during the observation period. (a) The fraction of trigger events that are actual earthquakes as the number of triggers increases, or the "true positive" rate. (b) The number of triggers on non-earthquakes, or "false positives", as the number of true positives increases. (c) The fraction of events that were missed, or "true negatives", of events in the catalog as the number of triggers increases. The color version of this figure is available only in the electronic edition.

signal and develops a quantitative parameter that is used to separate large- and small-magnitude earthquakes.

The three methods were applied to 34 catalog events that were successfully detected using nominal parameters with the simple threshold method. We assess whether the seismic signal a few seconds after the first break are correlated to the magnitude of the detected events. The first method (Fig. 8a) quantifies the frequency content of an earthquake from only a few seconds of data (Kanamori, 2005).

$$\tau_c = \frac{2\pi}{\sqrt{\frac{\int_0^{\tau_0} \dot{u}^2(t)\,dt}{\int_0^{\tau_0} u^2(t)\,dt}}}, \tag{1}$$

in which $u(t)$ is the ground-motion displacement, and τ_0 is the time window used for the analysis. The parameter τ_c is high for signals rich in higher frequency energy and low for signals dominated by lower frequency energy. The window τ_0 should be set to the minimum length of time necessary to ensure sufficient information about the frequency content. The second method that we tried uses the peak frequency, defined as the frequency corresponding to the value in a smoothed amplitude spectrum (Fig. 8b). Our third method uses the frequency index concept of (Buurman and West, 2006; Ketner and Power, 2013). This approach ratios the energy in a high-frequency band (1–5 Hz) by the energy in a low-frequency band (0–1 Hz) (Fig. 8c). All three approaches show some correlation with magnitude, but our limited data set shows no clear favorite in implementation. For example, all of the methods appear to be able to have the minimum value that could be set to divide earthquakes below and above around M_w 5, but none of them could be used to cleanly divide earthquakes above and below M_w 4. More testing is required to try to improve on the methodology of using the frequency content of a short time series. In the end, however, the implementation will likely still be imperfect, and it will have to be accepted that to skew the transmitted data to larger magnitude, farther away events, it will be necessary to accept that some mid-size (M_w 4–5) earthquakes may get cut short.

We also briefly consider how a network of a few stations separated by a few hundred kilometers might be used to autonomously differentiate between small and large events. A modest network cannot only increase the number of seismic event detections, but it can also give us a way to cross validate the detections and improve the chances of recording the most valuable signals.

(a) Threshold method number of triggers

(b) Segmented window method number of triggers

(c) Threshold method correct ratio

(d) Segmented window method correct ratio

Figure 7. Comparison of threshold detection method and segmented window detection method and the exploration of proper frequency of each method. Here, *x* axis is the upper limit of the band-pass filter applied to the data, and *y* axis represents the lower limit of the filter. Each dot in the figure is a combination of two parameters of a band-pass filter. (a,c) The threshold method and (b, d) the segmented window method. The panels (a) and (b) represents the number of triggers, and the panels (c) and (d) represents the ratio between correct detection and total number of triggers. The black stars indicate a seemingly best choice of the band-pass filter (2–8 Hz) for the segmented window method. The color version of this figure is available only in the electronic edition.

We consider the case in which three stations can communicate with a common orbiting computer that has the capability of turning data transmission on or off at each station. A computer on board the orbiter could be programmed for one station to tell the other stations to turn on after first triggering. If the other stations see nothing above some minimum noise level after the maximum possible travel time of a seismic wave between the two stations, then the evaluation could be made that the event was small and only observed at the initial station. Transmission could then be ceased at all stations to save power. As an initial test of this idea, we analyzed the seismic record from a handful of stations in the Alaska interior (Fig. 9a) at distances of 100–800 km from AK-SCRK to see how many of the events in our catalog were detectable in those more distal stations (Fig. 9b). The triggering algorithm that we used for this was the "segmented window" method using nominal parameters and the data filtered at 2–8 Hz. In our test, all of the common events detected by two or more stations that are farther than 5° (553 km) from each other are larger than M_w 3.5 (Fig. 9c).

Here again, our initial results show that the methodology has promise, so that this methodology combined with frequency content assessment may end up being highly effective at maximizing data collection from larger earthquakes. Further analyses

along the lines of Figure 9 may also be useful in mission design in terms of planning the station separation for a small network.

Discussion

The first seismometers to Venus will have a finite, limited power supply and little to no on-site data storage; these conditions present design challenges that are not present for lunar or Martian seismometer deployments. The series of short case studies that we conducted has provided some meaningful insights toward planning for future placement of a seismometer
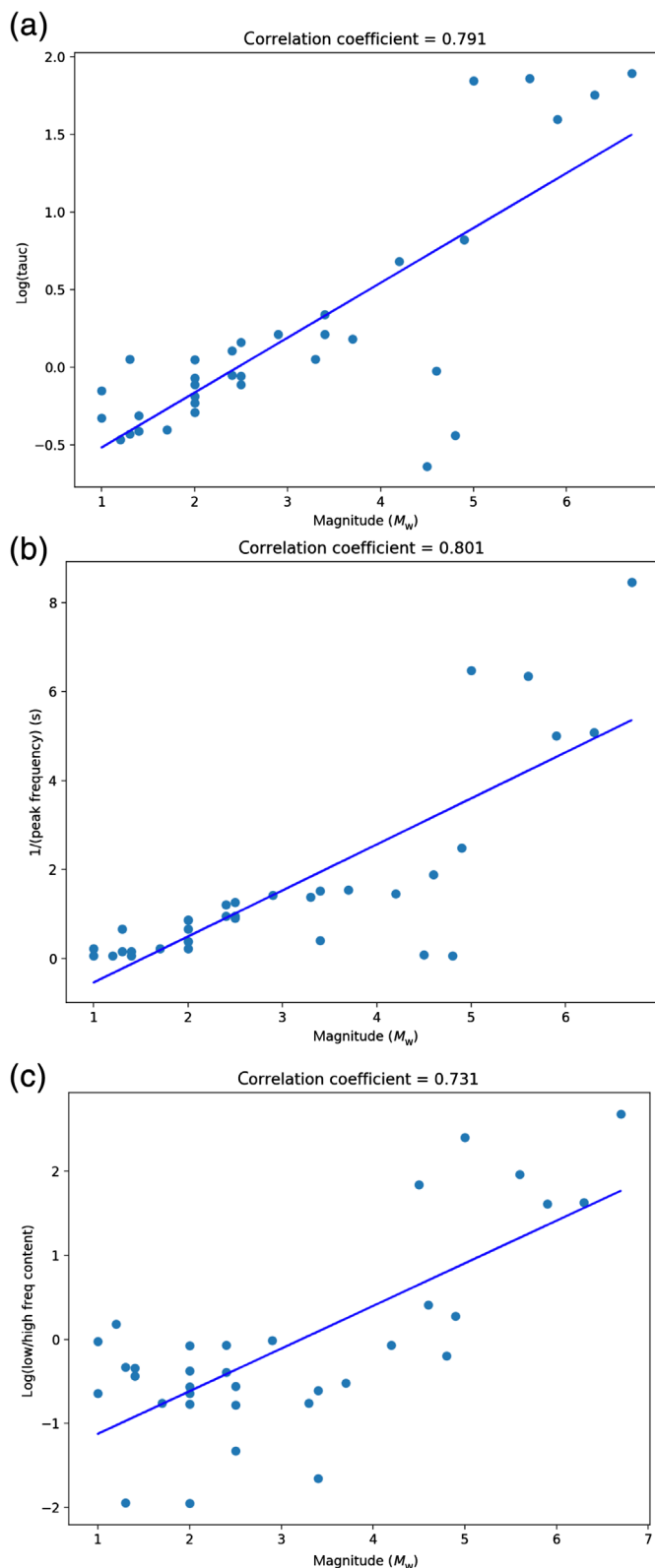
Figure 8. Correlation between earthquake magnitude and various frequency parameters. (a) τ_c, (b) peak frequency, and (c) frequency index. The color version of this figure is available only in the electronic edition.
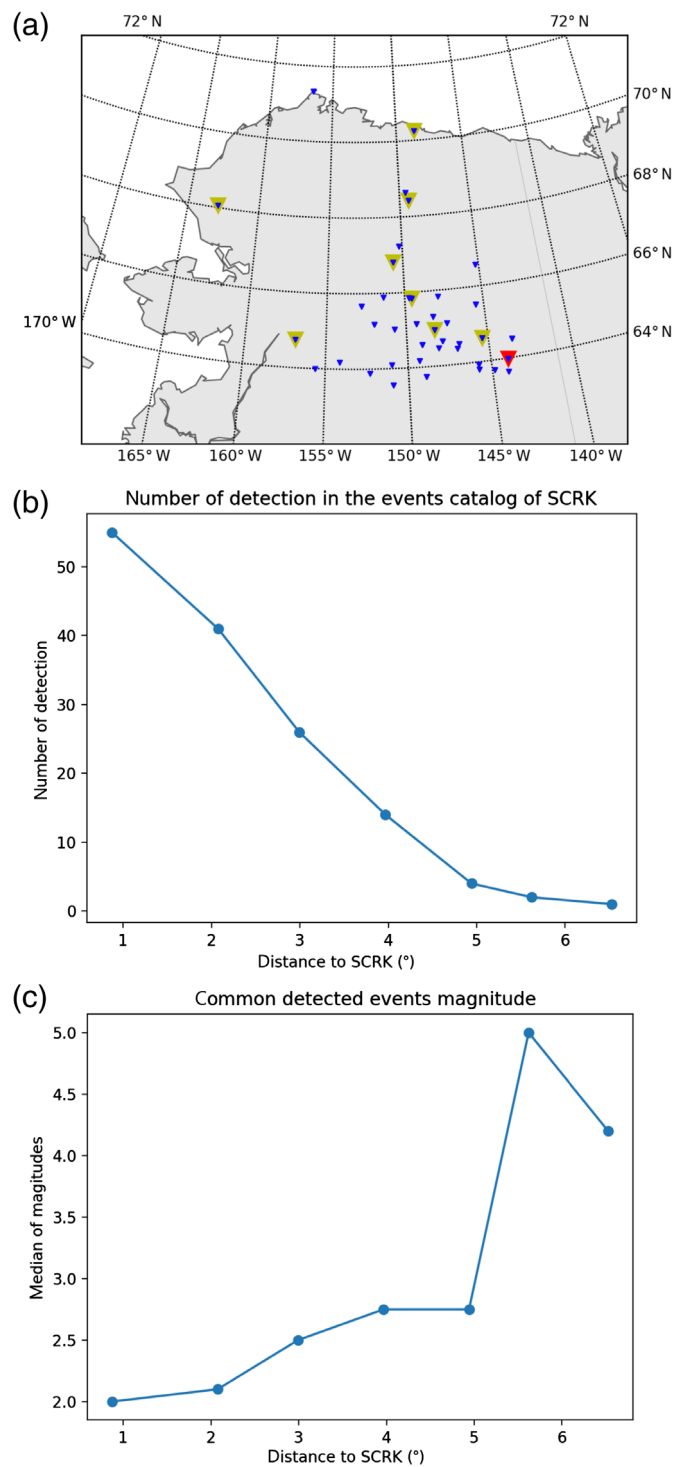
Figure 9. Small seismic station network test to rule out small nearby events. (a) The distribution of the selected stations. The red triangle is the AK-SCRK station; the green triangles are the stations in our analog network. (b) Number of detections on different distant stations. (c) The median magnitudes of common detected events in different stations in the network. The color version of this figure is available only in the electronic edition.

on Venus. An obvious caveat is that we have asserted that the station and seismic record that we used is typical of an intraplate setting, and that our observations have some universality. The observation that the most Venus-analogous places on Earth have seismicity levels that are within roughly an order of magnitude of mean Earth provides some confidence that our test station is reasonably representative of many Venus analog settings. Required future work is to repeat some of the tests using different time periods at the same station and using records from other stations in a variety of geographic and tectonic settings (especially the African plate), including in higher pressure environments such as below the ocean surface.

A fixed amount of battery power means that we must be selective of the data we choose to transmit. It is challenging to prevent a simple amplitude threshold trigger from triggering on small events without also frequently triggering on noise. Even if noise sources on Venus are "well-behaved" and vary in amplitude within a small range, without having a seismic record already in hand it would be educated guessing to preset the trigger level for the amplitude threshold method such that transmission was triggered on earthquakes and not noise.

However, with a method that relies on a ratio relative to noise level (either STA/LTA or "segmented window"), the negative outcome of guessing wrong on the expected level of seismicity will not be triggering on noise, but instead getting a less-than-desirable mix of low- versus high-amplitude events being transmitted. We have designed a seismicity detection method that comes close to matching the performance of an STA/LTA trigger and uses very limited memory and processing.

Regardless of the data transmission trigger that is chosen, it would clearly be beneficial if there were some ways to adjust the sensitivity of the trigger after seismometer deployment, even if just to be able to switch between a few different settings. If, for example, power limitations are such that the seismometer can monitor the surface for a few months but can only return a few hours of data, then we would desire a trigger sensitivity that results in transmitting, on average, an event every day or two. A trigger set to be too sensitive could expend the data transmission budget in just a few days and potentially before any large, distal earthquakes were observed. Conversely, an insensitive trigger might result in few or no events being transmitted back to Earth. We also tested various types of data filtering, and these can considerably improve trigger performance. In general terms, trigger performance at our test station was optimized with a band-pass of ~2–8 Hz. For a seismometer on Venus, transmitter power will limit data volume, which in turn means restrictions on dynamic range and sample rate. Thus, although innate instrument performance will dictate the lowest frequencies that the seismometer will transmit back to Earth, it is conceivable that the high-frequency cutoff for the transmitted data will be lower than the capability of the instrument. The more high-frequency content that can be included, the easier it is to distinguish small, nearby earthquakes from larger, farther away ones.

Our assessment of likely seismicity levels for Venus based on extrapolating the terrestrial record, and assuming that Venus must be more active than Mars, suggests that the most likely activity level that the first Venusian seismometers will observe will be around an order of magnitude less than Earth, but we should plan for a range of possibilities from the same to two orders of magnitudes less than global Earth. For comparison, the previous studies of Mars seismicity estimated a total moment release on Mars with about a fourth of Earth's surface area of 10^{17} N · m/yr to 10^{19} N · m/yr (Phillips, 1991; Golombek *et al.*, 1992; Knapmeyer *et al.*, 2006; Plesa *et al.*, 2018). The extrapolated global seismicity observed by InSight is close to these predictions, with the actual seismicity perhaps a few to several times greater than anticipated (Banerdt *et al.*, 2020).

The underlying premise of the STA/LTA trigger and our segmented window method is that noise sources do not generate abrupt spikes in ground motion. On Venus, noise is expected to result from near-surface winds, either directly or indirectly (a lengthy discussion of wind noise issues is in Lorenz, 2012). To maximize lander safety and the chance for the seismometer to deploy on a smooth surface to maximize coupling, the first seismometer on Venus will almost certainly deploy to locations with no discernable topography, places categorized as volcanic plains with surface slopes of <0.1° over thousands of square kilometers. With a solar day of 117 Earth days in duration, it is challenging to imagine situations that could generate sharp changes of wind speed at a lander location; the wind speed at the surface of Venus is expected to generally be <2 m/s (an overview of likely surface wind conditions is in Lorenz, 2016).

A more likely scenario is that some wind speed threshold is crossed that abruptly makes some lander part start rattling or flapping in an unanticipated way. It would be useful to have an independent wind monitor on the lander, and we expect that to be a part of future lander plans. However, a wind sensor would have the same problem as a seismometer of not being able to store or continuously transmit data. The wind sensor could be set to transmit data when the seismometer is transmitting, but that would only record the wind speed after triggering. A high wind speed and a seismic record characteristic of wind noise might allow an after-the-fact interpretation that a transmitted event was wind-caused. Figuring out how to incorporate a wind sensor into lander–orbiter operations in a way that prevents such an event from being transmitted is an area that requires additional research beyond the scope of this work.

The capability to have an orbiting spacecraft signal a seismometer to turn off data transmission would enable the ability to preferentially transmit for extended periods during major earthquakes and cut short transmission from small, nearby earthquakes. With an orbiter capable of onboard processing, over a short period the frequency content of the event can

be used to assess its likely magnitude. If an orbiting spacecraft can also turn on data transmission for a seismometer, then one seismometer can trigger others in a small network. Multiple stations make it easier to distinguish between large and small earthquakes, and a small network provides enormous advantages in terms of locating an earthquake, evaluating its magnitude, and using the event to infer subsurface properties.

Another advantage of an orbiter being able to turn on and turn off surface transmission is that the orbiter computer can have some capability to be reprogrammed to mitigate unanticipated problems on the lander. For example, if Venus proved to be much more seismically active than anticipated, so that many events are triggered per day at the lander, the orbiter could be set to rapidly shut down transmission of all but the largest earthquakes. In broader terms, if filtering or triggering mechanisms on the lander are not functioning as intended but can be turned on or off, then a programmable orbiter can help mitigate the problem by limiting the amount of undesired data that is transmitted. Of course, for a lander to be in continuous line-of-sight contact with an orbiter requires more than one orbiter, and potential mission scenarios could involve regular periods of time where an orbiter(s) will be out of contact with the lander. An additional use of an orbiter being able to send transmission on–off commands to the lander would be to put the lander in "stand-by" mode during periods, when the orbiter(s) is unable to communicate with it.

Although we think our test station is a reasonable analog for Venusian earthquake seismicity, it may not be a good analog for potential noise or coupling. A Venus seismometer will not be buried but instead will reside on the surface. We have tested the effect of wind noise on Earth, but the Venus atmosphere has a much higher density and pressure at the surface than on Earth, and conditions can be thought of as in between those for an ocean-bottom seismometer and one placed on the Earth's surface. Thus, testing comparison data from stations in similar tectonic settings (preferably near each other) collected by ocean-bottom seismometers and land-based seismometers is also part of our desired future work. In more general terms, repeating the initial studies presented here using stations in different locations on Earth, in different times, and in different noise settings to generalize our results is a high priority for future work.

Although it may seem fanciful to study seismic station operations on a planet for which we are a few years away from having an instrument prototype that can operate at Venus temperatures, these activities are providing key insights that are guiding instrument development. Our initial results suggest that finding a way to implement a segmented window trigger and the ability to turn on and off data transmission from orbit should be priorities for a Venus seismometer.

Data and Resources

The supplemental material available to this article includes the Venus analog seismicity catalog. It is also being used as the benchmarking catalog for testing detection algorithm (uploaded separately). The python code to generate the figures in the article are shared in GitHub link available at https://github.com/ytian159/Venus-Seismology (last accessed September 2022).

Declaration of Competing Interests

The authors acknowledge that there are no conflicts of interests recorded.

Acknowledgments

References

Banerdt, W. B., S. E. Smrekar, D. Banfield, D. Giardini, M. Golombek, C. L. Johnson, P. Lognonné, A. Spiga, T. Spohn, C. Perrin, *et al.* (2020). Initial results from the InSight mission on Mars, *Nature Geosci.* **13,** no. 3, 183–189, doi: 10.1038/s41561-020-0544-y.

Basilevsky, A. T., and J. W. Head (1995). Regional and global stratigraphy of Venus: A preliminary assessment and implications for the geological history of Venus, *Planet. Space Sci.* **43,** no. 12, 1523–1553.

Basilevsky, A. T., and J. W. Head (2002). Venus: Timing and rates of geologic activity, *Geology* **30,** no. 11, 1015–1018.

Burke, K. (1996). The African plate, *South Afr. J. Geol.* **99,** no. 4, 341–409, doi: 10.10520/EJC-942801f20.

Buurman, H., and M. E. West (2006). Seismic precursors to volcanic explosions during the 2006 eruption of Augustine volcano, in J. A. Power, M. L. Coombs, and J. T. Freymueller (Editors), *Chapter 2 in The 2006 Eruption of Augustine Volcano, Alaska*, U.S. Geological Survey, Alaska, U.S.A., 41–57, doi: 10.3133/pp17692.

Byrne, P. K., R. C. Ghail, A. M. C. Şengör, P. B. James, C. Klimczak, and S. C. Solomon (2021). A globally fragmented and mobile lithosphere on Venus, *Proc. Natl. Acad. Sci. Unit. States Am.* **118,** no. 26, doi: 10.1073/pnas.2025919118.

Crotwell, H. P., T. J. Owens, and J. Ritsema (1999). The TauP Toolkit: Flexible seismic travel-time and ray-path utilities, *Seismol. Res. Lett.* **70,** no. 2, 154–160.

Davaille, A., S. E. Smrekar, and S. Tomlinson (2017). Experimental and observational evidence for plume-induced subduction on Venus, *Nature Geosci.* **10,** no. 5, 349–355, doi: 10.1038/ngeo2928.

Didion, A., A. Komjathy, B. Sutin, B. Nakazono, A. Karp, M. Wallace, G. Lantoine, S. Krishnamoorthy, M. Rud, and J. Cutts (2018). Remote sensing of Venusian seismic activity with a small spacecraft, the VAMOS mission concept, *2018 IEEE Aerospace Conference, IEEE*, Big Sky, Montana, 3–10 March 2018, 1–14.

Foster, A., and F. Nimmo (1996). Comparisons between the rift systems of East Africa, Earth and Beta Regio, Venus, *Earth Planet. Sci. Lett.* **143,** no. 1, 183–195, doi: 10.1016/0012-821X(96)00146-X.

Giardini, D., P. Lognonné, W. B. Banerdt, W. T. Pike, U. Christensen, S. Ceylan, J. F. Clinton, M. van Driel, S. C. Stähler, M. Böse, *et al.* (2020). The seismicity of Mars, *Nature Geosci.* **13,** no. 3, 205–212, doi: 10.1038/s41561-020-0539-8.

Glass, D. E., J.-P. Jones, A. V. Shevade, D. Bhakta, E. Raub, R. Sim, and R. V. Bugga (2020). High temperature primary battery for Venus

surface missions, *J. Power Sources* **449,** 227,492, doi: 10.1016/j.jpowsour.2019.227492.

Golombek, M. P., W. B. Banerdt, K. L. Tanaka, and D. M. Tralli (1992). A prediction of Mars seismicity from surface faulting, *Science* **258,** no. 5084, 979–981.

Guest, J. E., and E. R. Stofan (1999). A new view of the stratigraphic history of Venus, *Icarus* **139,** no. 1, 55–66.

Herrick, R. R. (1999). Small mantle upwellings are pervasive on Venus and Earth, *Geophys. Res. Lett.* **26,** no. 6, 803–806.

Herrick, R. R., and M. E. Rumpf (2011). Postimpact modification by volcanic or tectonic processes as the rule, not the exception, for Venusian craters, *J. Geophys. Res. Planets* **116,** no. E2, doi: 10.1029/2010JE003722.

Johnson, C. L., and M. A. Richards (2003). A conceptual model for the relationship between coronae and large-scale mantle dynamics on Venus, *J. Geophys. Res. Planets* **108,** no. E6, doi: 10.1029/2002JE001962.

Kanamori, H. (2005). Real-time seismology and earthquake damage mitigation, *Annu. Rev. Earth Planet. Sci.* **33,** no. 1, 195–214, doi: 10.1146/annurev.earth.33.092203.122626.

Ketner, D., and J. Power (2013). Characterization of seismic events during the 2009 eruption of Redoubt volcano, Alaska, *J. Volcanol. Geotherm. Res.* **259,** 45–62.

Knapmeyer, M., J. Oberst, E. Hauber, M. Wählisch, C. Deuchler, and R. Wagner (2006). Working models for spatial distribution and level of Mars' seismicity, *J. Geophys. Res. Planets* **111,** no. E11, doi: 10.1029/2006JE002708.

Kremic, T., R. Ghail, M. Gilmore, G. Hunter, W. Kiefer, S. Limaye, M. Pauken, C. Tolbert, and C. Wilson (2020). Long-duration Venus lander for seismic and atmospheric science, *Planet. Space Sci.* **190,** 104,961, doi: 10.1016/j.pss.2020.104961.

Krishnamoorthy, S., A. Komjathy, J. A. Cutts, P. Lognonne, R. F. Garcia, M. P. Panning, P. K. Byrne, R. S. Matoza, A. D. Jolly, and J. B. Snively (2020). *Seismology on Venus With Infrasound Observations from Balloon and Orbit*, Sandia National Laboratory (SNL-NM), Albuquerque, New Mexico, U.S.A.

Lognonné, P., and C. Johnson (2007). Planetary seismology, *Treatise Geophys.* **10,** 69–122.

Lognonné, P., W. B. Banerdt, W. T. Pike, D. Giardini, U. Christensen, R. F. Garcia, T. Kawamura, S. Kedar, B. Knapmeyer-Endrun, L. Margerin, *et al.* (2020). Constraints on the shallow elastic and anelastic structure of Mars from InSight seismic data, *Nature. Geosci.* doi: 10.1038/s41561-020-0536-y.

Lorenz, R. D. (2012). Planetary seismology—Expectations for lander and wind noise with application to Venus, *Planet. Space Sci.* **62,** no. 1, 86–96.

Lorenz, R. D. (2016). Surface winds on Venus: Probability distribution from in-situ measurements, *Icarus* **264,** 311–315, doi: 10.1016/j.icarus.2015.09.036.

McGill, G. E., S. J. Steenstrup, C. Barton, and P. G. Ford (1981). Continental rifting and the origin of Beta Regio, Venus, *Geophys. Res. Lett.* **8,** no. 7, 737–740, doi: 10.1029/GL008i007p00737.

McKinnon, W. B., K. J. Zahnle, B. A. Ivanov, and H. J. Melosh (1997). Cratering on Venus: Models and observations, in S. W. Bougher, D. M. Hunten, and R. J. Philips (Editors), *Venus II Geology Geophysics,*

Atmosphere and Solar Wind Environment, University of Arizona Press, Tucson, Arizona, 969.

Megies, T., M. Beyreuther, R. Barsch, L. Krischer, and J. Wassermann (2011). ObsPy–What can it do for data centers and observatories? *Ann. Geophys.* **54,** no. 1, 47–58.

Mousavi, S. M., W. L. Ellsworth, W. Zhu, L. Y. Chuang, and G. C. Beroza (2020). Earthquake transformer—An attentive deep-learning model for simultaneous earthquake detection and phase picking, *Nat. Commun.* **11,** no. 1, 1–12.

Nakamura, Y., G. V. Latham, and H. J. Dorman (1982). Apollo lunar seismic experiment—Final summary, *J. Geophys. Res.* **87,** no. S01, A117–A123, doi: 10.1029/JB087iS01p0A117.

Okal, E. A., J. R. Sweet, S. Stein, and S. Mazzotti (2007). Frequency-size distributions for intraplate earthquakes, *Spec. Pap. Geol. Soc. Am.* **425,** 59–71, doi: 10.1130/2007.2425(05).

Phillips, R. (1991). Expected rate of marsquakes, in *Scientific Rationale and Requirements for a Global Seismic Network on Mars, LPI Tech. Rept. 91–02 LPI/TR-91–02*, Lunar and Planetary Institute, Houston, Texas, U.S.A., 35–38.

Plesa, A.-C., M. Knapmeyer, M. Golombek, D. Breuer, M. Grott, T. Kawamura, P. Lognonné, N. Tosi, and R. Weber (2018). Present-day mars' seismicity predicted from 3-D thermal evolution models of interior dynamics, *Geophys. Res. Lett.* **45,** no. 6, 2580–2589.

Sandwell, D. T., and G. Schubert (1992). Evidence for retrograde lithospheric subduction on Venus, *Science* **257,** no. 5071, 766–770, doi: 10.1126/science.257.5071.766.

Solomatov, V. S., and L.-N. Moresi (1996). Stagnant lid convection on Venus, *J. Geophys. Res. Planets* **101,** no. E2, 4737–4753.

Solomon, S. C., S. E. Smrekar, D. L. Bindschadler, R. E. Grimm, W. M. Kaula, G. E. McGill, R. J. Phillips, R. S. Saunders, G. Schubert, S. W. Squyres, *et al.* (1992). Venus tectonics: An overview of Magellan observations, *J. Geophys. Res. Planets* **97,** no. E8, 13,199–13,255.

Stevenson, D. J., J. A. Cutts, D. Mimoun, S. Arrowsmith, W. B. Banerdt, P. Blom, E. Brageot, Q. Brissaud, G. Chin, P. Gao, *et al.* (2015). *Probing the Interior Structure of Venus*, Keck Institute for Space Studies.

Tian, Y., and Y. Zheng (2020). AstroSeis: A 3D boundary element modeling code for seismic wavefields in irregular asteroids and bodies, *Seismol. Soc. Am.* **91,** no. 6, 3528–3538.

Trnkoczy, A. (2009). Understanding and parameter setting of STA/LTA trigger algorithm, in P. Bormann (Editor), *New Manual of Seismological Observatory Practice (NMSOP)*, Deutsches GeoForschungsZentrum GFZ, 1–20.

Turcotte, D. L. (1993). An episodic hypothesis for Venusian tectonics, *J. Geophys. Res. Planets* **98,** no. E9, 17,061–17,068, doi: 10.1029/93JE01775.

Venus Exploration Analysis Group (VEXAG) (2019). Venus Technology Plan, Lunar and Planetary Institute, available at https://www.lpi.usra.edu/vexag/documents/reports/VEXAG_Venus_Techplan_2019.pdf (last accessed September 2022).

Wassermann, J., L. Krischer, T. Megies, R. Barsch, and M. Beyreuther (2013). ObsPy: A Python toolbox for seismology, *Eos Trans. AGU* (Fall Meet. Suppl.), Abstracts S51A-2322.